

# Folding into a $\beta$ -Hairpin Can Prevent Amyloid Fibril Formation<sup>†</sup>

Waltteri Hosia,<sup>‡</sup> Niklas Bark,<sup>‡,§</sup> Edvards Liepinsh,<sup>‡</sup> Agneta Tjernberg,<sup>‡,||</sup> Bengt Persson,<sup>⊥,¶</sup> Dan Hallén,<sup>||</sup> Johan Thyberg,<sup>○</sup> Jan Johansson,<sup>‡,Ⓜ</sup> and Lars Tjernberg<sup>\*,+</sup>

Department of Medical Biochemistry and Biophysics, Karolinska Institutet, S-171 77 Stockholm, Sweden, Department of Clinical Neuroscience, Karolinska Institutet, S-171 77 Stockholm, Sweden, Department of Structural Chemistry, Biovitrum AB, S-112 76 Stockholm, Sweden, IFM, Bioinformatics, Linköping University, S-581 83 Linköping, Sweden, Centre for Genomics and Bioinformatics, Karolinska Institutet, S-171 77 Stockholm, Sweden, Department of Cell and Molecular Biology, Karolinska Institutet, S-171 77 Stockholm, Sweden, Department of Molecular Biosciences, Swedish University of Agricultural Sciences, The Biomedical Center, S-751 23 Uppsala, Sweden, and Department of Neurotec, Karolinska Institutet, S-141 57 Huddinge, Sweden

Received December 16, 2003; Revised Manuscript Received February 20, 2004

**ABSTRACT:** The tetrapeptide KFFE is one of the shortest amyloid fibril-forming peptides described. Herein, we have investigated how the structural environment of this motif affects polymerization. Using a turn motif (YNGK) or a less rigid sequence (AAAK) to fuse two KFFE tetrapeptides, we show by several biophysical methods that the amyloidogenic properties are strongly dependent on the structural environment. The dodecapeptide KFFEAAAKKFFE forms abundant thick fibril bundles. Freshly dissolved KFFEAAAKKFFE is monomeric and shows mainly disordered secondary structure, as evidenced by circular dichroism, NMR spectroscopy, hydrogen/deuterium exchange measurements, and molecular modeling studies. In sharp contrast, the dodecapeptide KFFEYNGKKFFE does not form fibrils but folds into a stable  $\beta$ -hairpin. This structure can oligomerize into a stable 12-mer and multiples thereof, as shown by size exclusion chromatography, sedimentation analysis, and electrospray mass spectrometry. These data indicate that the structural context in which a potential fibril forming sequence is present can prevent fibril formation by favoring self-limiting oligomerization over polymerization.

Amyloid fibrils are formed from specific proteins or peptides in several pathologic conditions, for example, Alzheimer's disease, Parkinson's disease, spongiform encephalopathies, and type II diabetes mellitus (1). Amyloid fibrils are composed of cross- $\beta$ -sheets (i.e., the constituent  $\beta$ -strands run perpendicular to the fiber axis (2)). However, the molecular-level mechanisms underlying the structural conversions required for fibril formation are not well-understood (3, 4). Although amyloid fibrils formed from different polypeptides have a very similar structure, the soluble forms of the polypeptides do not have major structural features in common. Changes in rate of aggregation of several fibril-forming polypeptides are correlated with a combination of changes in hydrophobicity, charge, and secondary structure propensity (3). For the amyloid  $\beta$ -peptide ( $A\beta$ )<sup>1</sup> found in the cerebral plaques associated with Alzheimer's disease, hydrophobicity was found to be a critical determinant for aggregation (5). Comparisons of three-dimensional structures of amyloidogenic proteins with their predicted structures

have identified certain  $\alpha$ -helices that are predicted to prefer  $\beta$ -strand structure. Such discordant regions appear to promote  $\alpha$ -helix to  $\beta$ -strand conversion and were suggested to be determinants for fibril formation (6, 7), a possibility supported by recent experiments (8).

Even stable globular proteins can aggregate into fibrils if they are incubated under partly denaturing conditions, suggesting that the fibrillar state can be populated by virtually all polypeptide chains (4, 9). However, the propensity to form fibrils under near-physiological conditions varies considerably between structurally similar peptides and between different regions with similar secondary structure of the same polypeptide chain. Even one-amino acid substitutions can change aggregation properties of a polypeptide dramatically (10–12). Differences in fibril formation have been correlated with relative rates of refolding and aggregation of the unfolded polypeptide chain (13, 14). Furthermore, certain regions of aggregating proteins have been found to be highly amyloidogenic. For example, in the disease-associated polypeptides  $A\beta$ , islet amyloid polypeptide, and tau, the sequences HQKLVFFAED, FGAIL, and VQIVYK, respectively, are crucial for polymerization of the corresponding full-length peptides (15–17).

Although increased  $\beta$ -strand propensity of polypeptide chains promotes fibril formation, the vast majority of  $\beta$ -sheet proteins are stable under physiological conditions and do not

<sup>†</sup> Supported by the Swedish Research Council, the Swedish Heart-Lung Foundation, the King Gustaf V 80th Birthday Fund, Tore Nilsons Stiftelse för Medicinsk Forskning, and Karolinska Institutet.

\* To whom correspondence should be addressed. E-mail: Lars.Tjernberg@neurotec.ki.se.

<sup>‡</sup> Department of Medical Biochemistry and Biophysics, Karolinska Institutet.

<sup>§</sup> Department of Clinical Neuroscience, Karolinska Institutet.

<sup>||</sup> Biovitrum AB.

<sup>⊥</sup> Linköping University.

<sup>¶</sup> Centre for Genomics and Bioinformatics, Karolinska Institutet.

<sup>○</sup> Department of Cell and Molecular Biology, Karolinska Institutet.

<sup>Ⓜ</sup> Swedish University of Agricultural Sciences.

<sup>+</sup> Department of Neurotec, Karolinska Institutet.

<sup>1</sup> Abbreviations:  $A\beta$ , amyloid  $\beta$ -peptide; CD, circular dichroism; EM, electron microscopy; ESI, electrospray ionization; HDX, hydrogen/deuterium exchange; MALDI, matrix assisted laser desorption ionization; PBS, phosphate buffered saline; SEC, size exclusion chromatography.

give rise to amyloid fibrils. A recent survey of  $\beta$ -sheet proteins showed that  $\beta$ -strands localized at the edges have features that prevent them from forming intermolecular sheets (18). This built-in negative design includes strategically placed prolines, charged residues, and geometries that disfavor interactions with other protein molecules. The effectiveness of some of these features was experimentally verified by introduction of Lys residues that converted fibrillogenic polypeptides into soluble  $\beta$ -sheet proteins (19). Short polypeptides, accessible to a variety of experimental systems, have been used to correlate structure and fibril formation. We have shown that both charge attraction and  $\beta$ -strand propensity are crucial for amyloid formation from the tetrapeptide KFFE, one of the shortest fibril-forming peptides so far described (20). KFFE shows a mixture of  $\beta$ -strand and nonordered structure in solution. Herein, we studied the 12-residue peptides KFFEYNGKKFFE (including the strong turn motif YNGK (21, 22)) and KFFEAAKKFFE (turn motif replaced by AAK) in an attempt to determine how fibril formation of the tetrapeptide segment KFFE is influenced by its structural context.

## MATERIALS AND METHODS

**Peptides and Incubations.** Peptides, purified by reversed-phase HPLC, were purchased from Interactiva (Darmstadt, Germany). The identities of the peptides were verified with electrospray ionization (ESI) mass spectrometry. The peptides were incubated at 10–3000  $\mu$ M concentration for 0–22 days at 37 °C in 50 mM phosphate buffered saline (PBS), pH 7.4, or in unbuffered water, pH 5.5.

**Electron Microscopy (EM).** After the incubation periods, the peptide solutions were either directly applied to EM grids covered by a Formvar film, or centrifuged at 20 000g for 30 min, whereafter pelleted material was suspended in 40  $\mu$ L of water by low-energy sonication for 5 s. Aliquots of 8  $\mu$ L were applied to the EM grids, excess fluid was withdrawn after 30 s, and after air-drying the grids were negatively stained with 1.5% uranyl acetate in water. The stained grids were examined and photographed in a Philips CM120TWIN electron microscope operated at 80 kV.

**Circular Dichroism (CD) Spectroscopy.** Peptides were dissolved at 300  $\mu$ M in sodium phosphate buffer, pH 7.0, or in distilled water. Immediately after solubilization, CD spectra between 260 and 180 nm were recorded at 20 °C using an AVIV Model 5 62DS spectropolarimeter (Jacksonville, NJ). Samples incubated as described previously were analyzed using the same parameters. For samples containing trifluoroethanol, 2 mM stock solutions of peptides were diluted to 200  $\mu$ M in 10–80% aqueous trifluoroethanol. To compensate for the contributions of the phenylalanine side chains, the CD spectrum of the dipeptide FF was subtracted from the spectra. Residual molar ellipticity was calculated from peptide concentrations determined by amino acid analysis and is expressed in kdeg cm<sup>2</sup>/dmol.

**Mass Spectrometry (MS).** For hydrogen/deuterium exchange (HDX) measurements, 1  $\mu$ L solutions of KFFEYNGKKFFE and KFFEAAKKFFE, each of 2 mM, were mixed, and the volume was reduced under a stream of nitrogen to approximately 0.5  $\mu$ L. Then 198  $\mu$ L of D<sub>2</sub>O (99.8% D atoms, Sigma-Aldrich) and 1  $\mu$ L of CH<sub>3</sub>COOD (99.8% D atoms, Eur-isotope, France) were added, giving a

final deuterium content of  $\geq 99\%$  and a total peptide concentration of 20  $\mu$ M. The peptide mixture was incubated at 22 °C, and aliquots were removed for analysis at different time points. All handling was conducted in a closed hood flushed with nitrogen. Three samples were analyzed for each time point. The samples were spotted on to a predried matrix of deuterated  $\alpha$ -cyano cinnamic acid (13). A Voyager De-Pro MALDI-TOF instrument (Perceptive Biosystems Inc.) operated in the linear mode was employed for matrix-assisted laser desorption ionization (MALDI) mass measurements.

For the study of oligomer formation, nondenaturing ESI was employed. The peptide KFFEYNGKKFFE (300  $\mu$ M) was incubated in 10 mM ammonium acetate, pH 7, for 2 weeks prior to analysis. The sample was diluted to 50  $\mu$ M with 10 mM ammonium acetate, pH 7, and 5  $\mu$ L was injected into the MS system at a flow rate of 5  $\mu$ L/min. Mass spectra were recorded on a Q-TOF Ultima API instrument (Micro-mass, Manchester, UK), operating in positive ion mode. The instrument conditions for the ESI interface were as follows: capillary voltage 3000 V, cone voltage 100 V, source block temperature 60 °C, desolvation temperature 80 °C, desolvation gas flow 400 L/h, and nebulizer gas flow 100 L/h. An elevated instrument pressure in the source region, as well as collisional cooling, was applied to preserve noncovalent interactions in the gas phase. Ions were scanned from  $m/z$  1000–5000, with data accumulation of 2 s per spectrum and an interscan time delay of 0.1 s. The mass spectra were averaged over 25 scans.

**NMR Spectroscopy.** NMR measurements of 0.2 mM concentrations of KFFEYNGKKFFE and KFFEAAKKFFE were performed at pH 5.5, unbuffered, and  $t = 25$  °C in 95% H<sub>2</sub>O/5% D<sub>2</sub>O on a Bruker DMX 600 spectrometer equipped with a cryoprobe. Assignments of signals were done in a standard way by using homonuclear NOESY (mixing time 300 ms) and TOCSY (mixing time 60 ms) spectra and analyzed with the help of the program XEASY. <sup>1</sup>H signal assignments were confirmed with <sup>13</sup>C-<sup>1</sup>H HSQC spectra taken at natural abundance of <sup>13</sup>C isotope.

**Size Exclusion Chromatography (SEC).** SEC was performed on a Superose 12 HR 10/30 column (Amersham Bioscience, Uppsala, Sweden) with PBS, pH 7.4, or 50 mM ammonium acetate, pH 7.0, as mobile phase at a flow rate of 0.8 mL/min. Absorbance was measured at 257 nm. Peptides incubated in either PBS or water were analyzed immediately after dissolution and after 3, 7, 14, or 22 days of incubation. Collected peaks were lyophilized or stored at –80 °C prior to further analysis.

**Analytical Ultracentrifugation.** The sedimentation velocity experiment was performed with a Beckman Optima XL-I using interference optical detection system. Epon double-sector centerpieces were filled with 400  $\mu$ L of 0.6 mM peptide in PBS pH 7.4. Experiments were performed at a rotor speed of 50 000 rpm at 20 °C. The data were analyzed applying the Lamm equation on sedimentation using the program SEDFIT (23) to obtain a concentration distribution of sedimentation coefficients. In the calculation, 350 scans were used.

**Molecular Modeling.** Ab initio predictions were performed using the ICM program (version 3.0, Molsoft LLC, La Jolla, CA) with the biased probability Monte Carlo method (24). For each peptide, six independent modeling rounds were

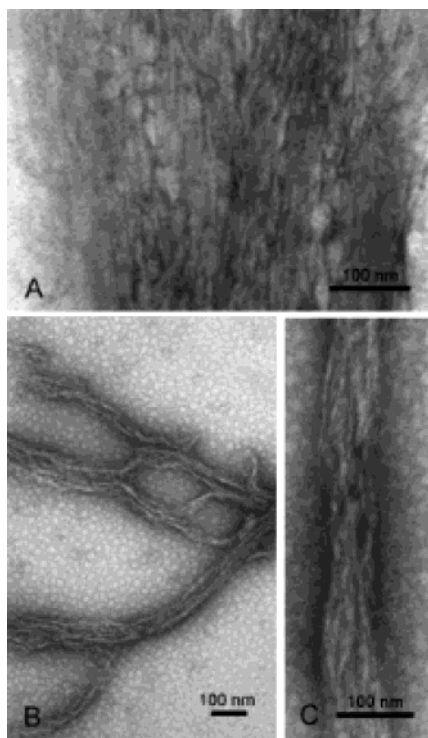


FIGURE 1: Amyloid fibrils formed by KFFEAAAKKFFE incubated at 400  $\mu$ M in PBS for 20 days (A) or at 3 mM in water for 10 days (B and C).

undertaken, and the lowest energy conformations were compared.

**Data Base Search for Structural Motifs.** All structures, after removal of sequence homologues, containing AAAK, YNGK, or KFFE tetrapeptide segments were downloaded from the Protein Data Bank. The structures were visualized using Swiss-PdbViewer, and the secondary structures of the regions were determined by inspection. Structures lacking tertiary structure data for the regions of interest were excluded.

## RESULTS

**Fibril Formation.** KFFEAAAKKFFE and KFFEYNGKKFFE showed distinctly different polymerization behavior as observed by EM. Even at the lowest concentration studied, 10  $\mu$ M, KFFEAAAKKFFE formed fibrils, although at moderate amounts. Incubation of KFFEAAAKKFFE at 400  $\mu$ M or 3 mM concentration yielded abundant thick fibril bundles (Figure 1). KFFEYNGKKFFE did not form amyloid-like fibrils under any of the conditions employed. In some samples, small networks of short fibrillar fragments could be observed. The differences in fibril formation between KFFEAAAKKFFE and KFFEYNGKKFFE were corroborated by staining with Thioflavin T. KFFEAAAKKFFE incubated at 3 mM concentration in PBS for 6 days gave a 4-fold increase in ThT fluorescence, while KFFEYNGKKFFE under the same conditions only gave about 30% increase in fluorescence (data not shown).

**Secondary Structure.** CD spectroscopy of freshly dissolved KFFEYNGKKFFE showed a broad minimum around 215 nm and a maximum at about 195 nm, indicating the presence of mainly  $\beta$ -strand structure (Figure 2). Addition of 10–80% (v/v) trifluoroethanol gave rise to a slightly more

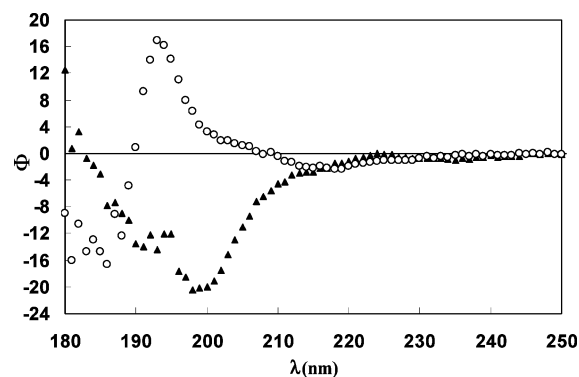


FIGURE 2: CD spectra of KFFEAAAKKFFE (filled triangles) and KFFEYNGKKFFE (open circles) peptides at a concentration of 100  $\mu$ M in water.

pronounced minimum at 215 nm but no other changes. Freshly dissolved KFFEAAAKKFFE showed a distinctly different CD spectrum as compared to that of KFFEYNGKKFFE (Figure 2). The KFFEAAAKKFFE spectrum showed a deep minimum at about 200 nm, and a broad maximum around 225 nm, which is typical for an unordered structure. Addition of 10–80% (v/v) trifluoroethanol to KFFEAAAKKFFE gradually changed the spectra so that a minimum around 218–219 nm combined with a minimum around 205 nm was obtained (data not shown). This shows that KFFEAAAKKFFE, unlike KFFEYNGKKFFE, changes its structure in the presence of high concentrations of trifluoroethanol.

The results from CD analysis were supported by NMR measurements (chemical shifts are given in Tables 1 and 2 of the Supporting Information). Both KFFEYNGKKFFE and KFFEAAAKKFFE showed big  $^3J(\text{HNC}_\alpha\text{H})$  coupling constants ( $>8$  Hz) for the first four and the last four amino acid residues. This was especially notable for KFFEYNGKKFFE and supports a predominantly extended structure of this peptide in solution. Additionally, for KFFEYNGKKFFE (but not for KFFEAAAKKFFE) the NOESY spectrum displayed, besides the usual sequential HN–HN connectivities typical for small peptides at 300 ms mixing time, two unambiguous interstrand HN–HN NOEs: Tyr5–Lys8 and Phe3–Phe10 (Figure 3). This indicates that KFFEYNGKKFFE is either folded intramolecularly or that it forms a dimeric structure. Unambiguous indication that the peptide is folded came from analysis of coupling constant values of Gly7:  $^3J(\text{HNC}_\alpha\text{H}_1) = ^3J(\text{HNC}_\alpha\text{H}_2) = 5.5$  Hz and  $^2J(\text{C}_\alpha\text{H}_1\text{C}_\alpha\text{H}_2) = 17.2$  Hz. These couplings taken together (25) strongly support that Gly7 residue is not in extended conformation as it should be in case of a dimer but that it together with Asn6 forms a  $\beta$ -turn. For KFFEAAAKKFFE, the  $^3J(\text{HNC}_\alpha\text{H})$  coupling constants for residues 5–8 are typical of random coil structure ( $\sim 6.5$  Hz). These conclusions were confirmed by chemical shift analysis for  $\text{C}_\alpha\text{H}$  protons in both peptides as compared to random coil values (26) (Table 1). Significant low field shifts in case of KFFEYNGKKFFE as compared to random coil values are in agreement with predominant antiparallel  $\beta$ -sheet formation. KFFEAAAKKFFE displayed  $\text{C}_\alpha\text{H}$  shifts close to random coil values for all residues except 2 and 11.

**HD Exchange.** The flexibility of KFFEAAAKKFFE and KFFEYNGKKFFE was investigated by HDX combined with MALDI-MS. Figure 4 shows the number of shielded protons



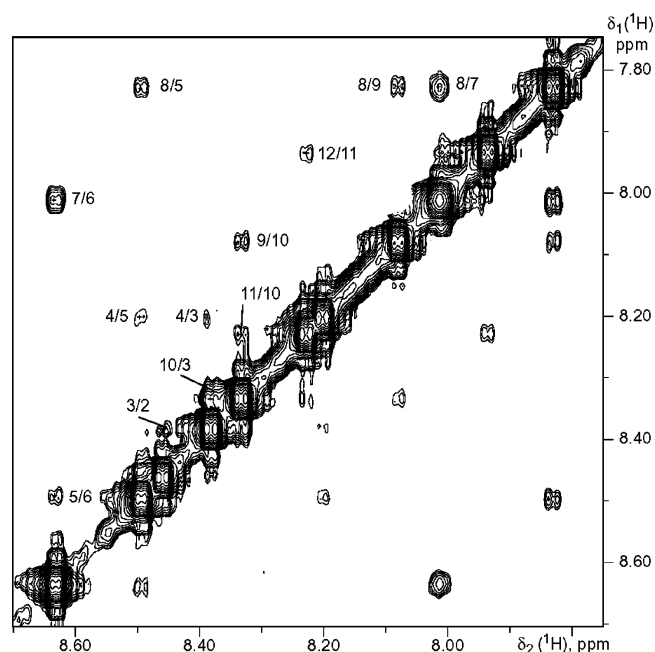


FIGURE 3: Part of the NOESY spectrum of KFFEYNGKKFFE peptide showing NH–NH connectivities. All sequential connectivities are weak except N6–G7 and G7–K8, indicating the presence of a turn. Antiparallel orientation of N- and C-termini are confirmed by the long-range NOEs Y5–K8 and F3–F10.

Table 1: NMR Shift Difference for C<sub>α</sub>H Protons between Peptide and Random Coil (26) Values

residue	KFFEYNGKKFFE	residue	KFFEAAAKKFFE
1 (K)	−0.33	1 (K)	−0.36
2 (F)	+0.51	2 (F)	+0.18
3 (F)	+0.12	3 (F)	+0.03
4 (E)	+0.39	4 (E)	−0.10
5 (Y)	+0.13	5 (A)	−0.02
6 (N)	−0.22	6 (A)	−0.06
7 (G)	+0.03/−0.20	7 (A)	−0.06
8 (K)	+0.09	8 (K)	−0.10
9 (K)	+0.09	9 (K)	−0.06
10 (F)	+0.10	10 (F)	+0.09
11 (F)	+0.24	11 (F)	+0.11
12 (E)	−0.05	12 (E)	+0.08

as a function of time for the two peptides coincubated in D<sub>2</sub>O containing 0.5% (v/v) CH<sub>3</sub>COOD. KFFEYNGKKFFE maintains three to four shielded hydrogens, while the exchange in KFFEAAAKKFFE was almost complete. Addition of 50% (v/v) acetonitrile resulted in practically complete exchange for both peptides, while addition of 150 mM sodium chloride had no significant effect on the number of shielded hydrogens (data not shown).

**Molecular Modeling.** Taken together, the CD, NMR, and HDX data strongly suggest that KFFEYNGKKFFE forms a strand (residues 1–5) turn (residues 6 and 7) strand (residues 8–12)  $\beta$ -hairpin structure. This structure is stabilized by hydrophobic interactions to a significant extent, while ionic interactions play a minor role, as judged from the HDX data. In line with these results, the lowest energy conformation from molecular modeling of the KFFEYNGKKFFE peptide showed a  $\beta$ -hairpin structure (Figure 5). Also, the second best conformation (with 3.7 kcal/mol higher energy) revealed a  $\beta$ -hairpin structure. The CD, NMR, and HDX data show that KFFEAAAKKFFE is structurally unordered. The lowest energy conformation for KFFEAAAKKFFE showed a central

helix part and flanking coil regions. The second best conformation, with 1.3 kcal/mol higher energy, showed large similarities with the lowest energy conformation.

**Quaternary Structure of KFFEYNGKKFFE.** The stable  $\beta$ -hairpin structure of KFFEYNGKKFFE would suggest that it is capable of forming intermolecular  $\beta$ -sheet structure and fibrils (21). The apparent lack of significant fibril formation prompted us to investigate whether alternative modes of polymerization occur for KFFEYNGKKFFE. Analysis by SEC showed that KFFEYNGKKFFE undergoes oligomerization into a structure of a defined size over the course of two weeks when incubated in PBS at 37 °C (Figure 6, first column). No formation of oligomers was observed when KFFEYNGKKFFE was incubated in unbuffered water, pH 5. KFFEAAAKKFFE did not show any sign of oligomerization (Figure 6, second column). Lyophilization of collected fractions did not alter the elution time, when reinjected onto the column. The oligomers were also resistant to heating (80 °C for 30 min) and low pH (pH 2.5 for 3 days) (data not shown).

The nature of KFFEYNGKKFFE oligomers was further studied by ESI-MS and sedimentation analysis. From the concentration sedimentation distribution, we could identify four species containing the peptide at 1.91, 3.11, 3.96, and 4.98 S (Figure 7). On the basis of the friction ratio,  $f/f_0 = 1.23$ , obtained from the analysis, this would best correspond to aggregates consisting of 12, 24, 48, and 60 peptides, respectively. Nondenaturing ESI mass spectrometry likewise revealed the presence of oligomers in KFFEYNGKKFFE samples incubated for 2 weeks in 10 mM ammonium acetate (Table 2). The  $m/z$  peak at 1902 Da is unique for a hexamer and multiples thereof. The reason for possible dissociation of a 12-mer in the mass spectrometer is probably due to weakening of hydrophobic interactions when the complex is transferred into the gas phase.

## DISCUSSION

This work extends our previous report of amyloid fibril formation by the tetrapeptides KFFE and KVVE, showing that charge attraction (lysine–glutamic acid) and high  $\beta$ -strand propensity (phenylalanines or valines) are essential for fibril formation (20). In another recent study, the formation of intramolecular  $\beta$ -strands, induced by the turn motif YNGK, was found to promote fibril formation of A $\beta$ -derived peptides (21). Here, we combine the KFFE sequence and the turn motif into the dodecapeptide sequence KFFEYNGKKFFE, resulting in a stable  $\beta$ -hairpin. This is, to the best of our knowledge, the shortest peptide with a defined stable  $\beta$ -hairpin structure. Interestingly, KFFEYNGKKFFE did not form fibrils, even when incubated several weeks at high concentration. Instead, 12-mers (and multiples thereof) were formed. Since these 12-mers do not polymerize into fibrils, we conclude that this oligomer is a self-limiting structure.

On the other hand, connecting two KFFE sequences with a more flexible hinge, KFFEAAAKKFFE, resulted in a less structured but more amyloidogenic peptide. We suggest that KFFEAAAKKFFE forms intermolecular contacts from an open conformation, forming in register and/or staggered polymers. In this case, the peptide can participate in eight backbone hydrogen bond pairs (not counting bonds formed

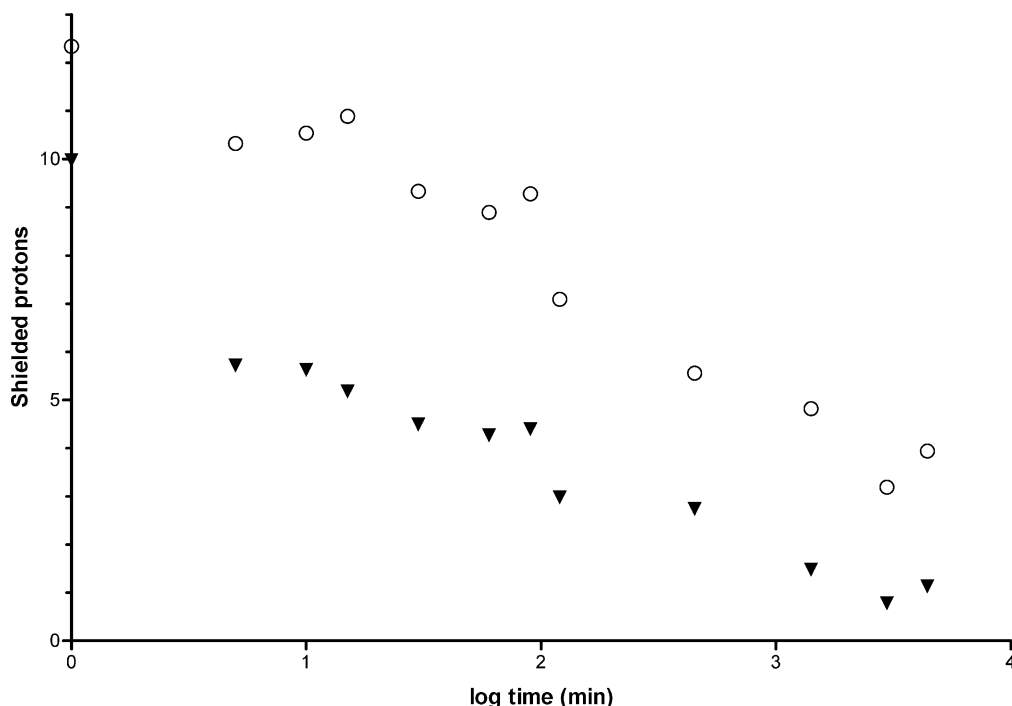


FIGURE 4: Hydrogen/deuterium exchange of KFFEAAAKKFFE (filled triangles) and KFFEYNGKKFFE (open circles) peptides in 0.5% (v/v)  $\text{CH}_3\text{COOD}$  in  $\text{D}_2\text{O}$  at 22 °C, as observed by MALDI mass spectrometry. The number of shielded (i.e., nonexchanged) hydrogen atoms are plotted vs time.

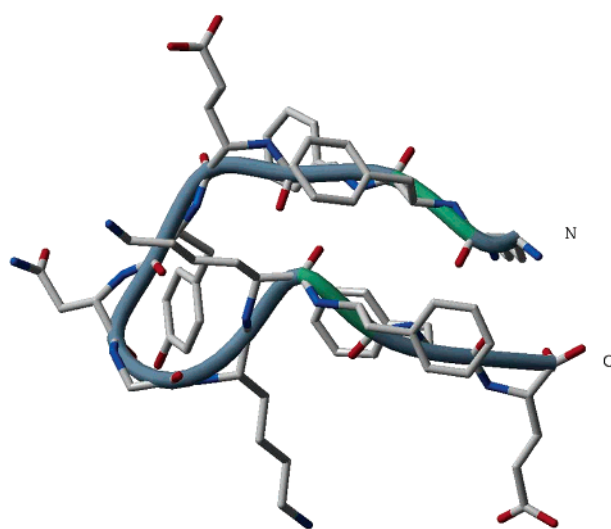


FIGURE 5: Molecular modeling of the KFFEYNGKKFFE peptide. The modeling was started from an open structure. The lowest energy conformation obtained from six different experiments is shown. The  $\beta$ -hairpin structure is in accordance with data from CD, NMR, and HDX experiments.

by the AAAK motif) involving neighboring peptides. Thus, by connecting two amyloidogenic KFFE sequences, the tendency to form fibrils was highly increased. The markedly lower amyloidogenicity of KFFEYNGKKFFE as compared to KFFEAAAKKFFE may be explained by the fact that the  $\beta$ -hairpin allows the two KFFE motifs to form a maximum of four intermolecular backbone hydrogen bond pairs with other molecules. However, the tetrapeptide KFFE forms fibrils (20) but no detectable oligomers, and the tendency of KFFEYNGKKFFE to form 12-mers instead of fibrils must thus stem from the presence of the YNGK turn motif. The induced conformation could be regarded as an example of negative design, a term introduced to describe how proteins

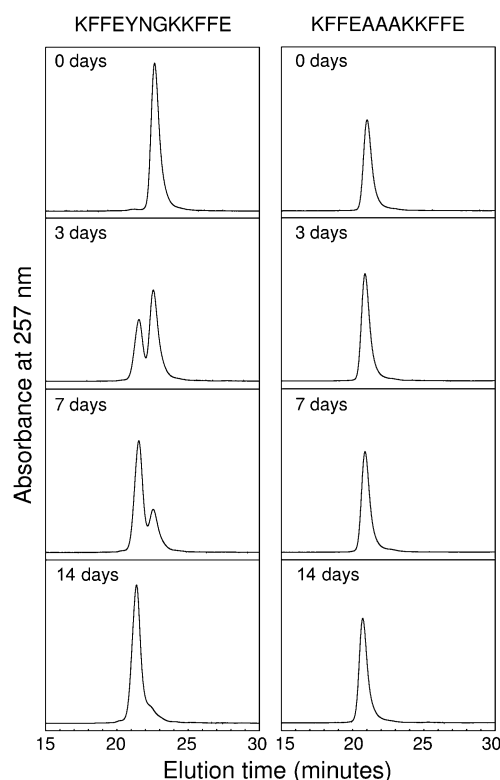


FIGURE 6: Size exclusion chromatography. KFFEYNGKKFFE (left column) or KFFEAAAKKFFE (right column) were incubated for the indicated time periods in PBS at 37 °C prior to injection. KFFEYNGKKFFE showed a complete conversion to a larger species within 14 days of incubation, while KFFEAAAKKFFE showed no sign of oligomerization.

avoid self-aggregation by charged residues or bulges in exposed  $\beta$ -strands (18). YNGK motifs can be found in 22 nonredundant structures deposited in the Protein Data Bank (Table 3). Fifteen of these motifs form turn structures, 11 of

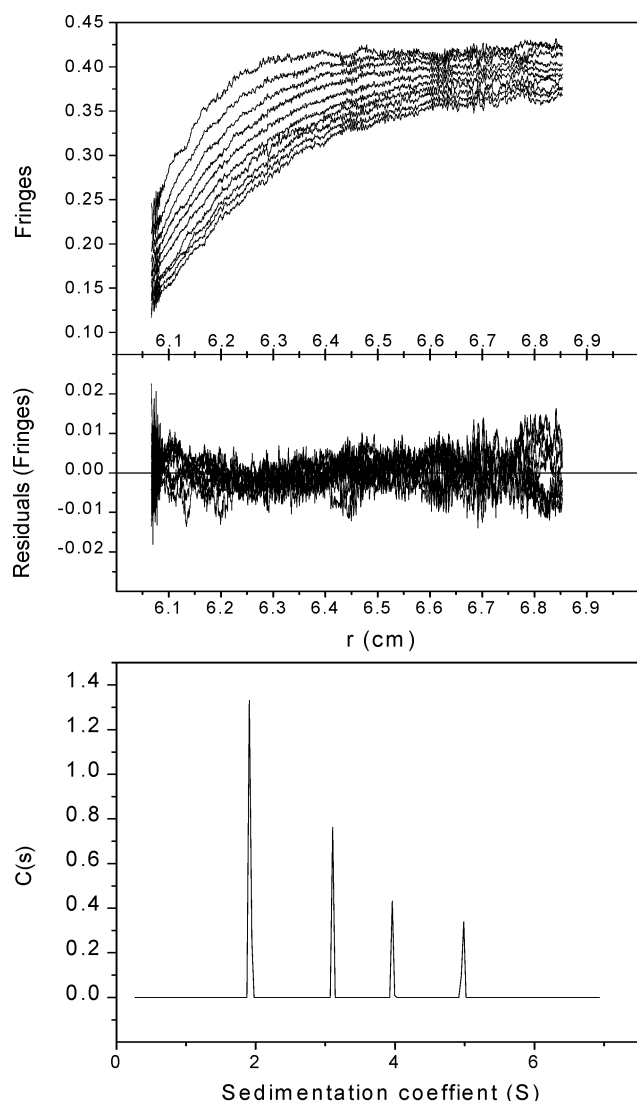


FIGURE 7: Analytical ultracentrifugation analysis of the peptide KFFEYNGKKFFE. The top panel shows raw sedimentation velocity radial scan data obtained at 50 000 rpm. For clarity, the plot shows every 20 in the scan range 40–220. The data are presented as fringes displacements, which is proportional to the peptide concentration, plotted against the distance from the axis of rotation. The middle panel shows the residuals after fitting to a continuous concentration vs sedimentation coefficient,  $c(s)$ , model. The rmsd for the fit was 0.0054 fringes. The bottom panel shows the distribution of sedimentation coefficients obtained from the sedimentation velocity data. Data analysis was performed using the program SEDFIT.

which are nearly identical to the turn present in our proposed structure of a KFFEYNGKKFFE hairpin (Figure 5). Hence, the strong tendency of YNGK to form a  $\beta$ -hairpin minimizes the risk of misfolding and aggregation of these proteins. We suggest that YNGK and similar motifs are of importance for protein folding by rapidly closing potential amyloidogenic sequences.

By differently combining short (four residues) building blocks, it is possible to construct peptides with widely varying characteristics. Combining the  $\beta$ -sheet motif KFFE with the turn motif YNGK resulted in a stable  $\beta$ -hairpin that assembled into a 12-mer. Connecting the  $\beta$ -sheet motif with the AAAK sequence resulted in a peptide that aggregated into long fibril bundles. We suggest that the blocks described here, together with similar short blocks with different prop-

Table 2: Possible Oligomeric Assemblies Compatible with the Found  $m/z$  Ratios<sup>a</sup>

$m/z$	monomer	dimer	trimer	tetramer	pentamer	hexamer
1057.0		<b>3+</b>		6+		9+
1188.8			<b>4+</b>			8+
1268.1				<b>5+</b>		
1584.7	<b>1+</b>	2+	3+	4+	5+	6+
1901.6						<b>5+</b>
2112.9				<b>3+</b>		
2377.3			<b>2+</b>			4+

<sup>a</sup> Observed  $m/z$  peaks from an ESI-MS spectrum after analysis of KFFEYNGKKFFE incubated for 2 weeks in ammonium acetate. The MS analysis was performed under nondenaturing conditions to preserve the noncovalent binding interactions in the gas phase. Numbers indicate the charge state of the corresponding oligomer in the table head. Bold numbers indicate the smallest possible oligomer consistent with the found  $m/z$ .  $m/z = 1902$  is unique for a hexamer (or multiples thereof).

Table 3: Secondary Structure of the Tetrapeptide Motifs Found in the Protein Data Bank

sequence	$\alpha$ -helix	$\beta$ -sheet	$\beta$ -turn	other	total
YNGK	0	0	15	7	22
AAAK	79	0	1	17	97
KFFE	4	2	0	1	7

erties, could be used for design of small functional polypeptides or modifications of naturally occurring proteins.

Minor changes in primary structure can have prominent effects on peptide aggregation (27, 28). Studies with model peptides show that  $\beta$ -sheet formation and increased length of the  $\beta$ -strand motif increase the tendency to aggregate (29). Our data support these results insofar as the dodecapeptide KFFEAAAKKFFE forms more abundant and larger fibrils than the KFFE tetrapeptide. However, intramolecular  $\beta$ -strand formation in the KFFEYNGKKFFE peptide practically abolished fibril formation. The presence of a fibril-forming sequence motif in a polypeptide chain may thus result in very different oligomerization/polymerization propensities depending on the structural context.

## SUPPORTING INFORMATION AVAILABLE

Resonance assignments for the KFFEYNGKKFFE and KFFEAAAKKFFE peptides. This material is available free of charge via the Internet at <http://pubs.acs.org>.

## REFERENCES

1. Rochet, J. C., and Lansbury, P. T., Jr. (2000) Amyloid fibrillogenesis: themes and variations, *Curr. Opin. Struct. Biol.* 10, 60–68.
2. Sunde, M., and Blake, C. C. (1998) From the globular to the fibrous state: protein structure and structural conversion in amyloid formation, *Q. Rev. Biophys.* 31, 1–39.
3. Chiti, F., Stefani, M., Taddei, N., Ramponi, G., and Dobson, C. M. (2003) Rationalization of the effects of mutations on peptide and protein aggregation rates, *Nature* 424, 805–808.
4. Dobson, C. M. (1999) Protein misfolding, evolution and disease, *Trends Biochem. Sci.* 24, 329–332.
5. Wurth, C., Guimard, N. K., and Hecht, M. H. (2002) Mutations that reduce aggregation of the Alzheimer's Abeta42 peptide: an unbiased search for the sequence determinants of Abeta amyloidogenesis, *J. Mol. Biol.* 319, 1279–1290.
6. Dima, R. I., and Thirumalai, D. (2002) Exploring the propensities of helices in PrP(C) to form  $\beta$ -sheet using NMR structures and sequence alignments, *Biophys. J.* 83, 1268–1280.

7. Kallberg, Y., Gustafsson, M., Persson, B., Thyberg, J., and Johansson, J. (2001) Prediction of amyloid fibril-forming proteins, *J. Biol. Chem.* 276, 12945–12950.
8. Thirumalai, D., Klimov, D. K., and Dima, R. I. (2003) Emerging ideas on the molecular basis of protein and peptide aggregation, *Curr. Opin. Struct. Biol.* 13, 146–159.
9. Fandrich, M., Fletcher, M. A., and Dobson, C. M. (2001) Amyloid fibrils from muscle myoglobin, *Nature* 410, 165–166.
10. Damas, A. M., and Saraiva, M. J. (2000) Review: TTR amyloidosis-structural features leading to protein aggregation and their implications on therapeutic strategies, *J. Struct. Biol.* 130, 290–299.
11. Van Broeckhoven, C., Haan, J., Bakker, E., Hardy, J. A., Van Hul, W., Wehnert, A., Vegter-Van der Vlis, M., and Roos, R. A. (1990) Amyloid beta protein precursor gene and hereditary cerebral hemorrhage with amyloidosis (Dutch), *Science* 248, 1120–1122.
12. Takahashi, Y., Ueno, A., and Mihara, H. (2000) Mutational analysis of designed peptides that undergo structural transition from  $\alpha$ -helix to  $\beta$ -sheet and amyloid fibril formation, *Structure* 8, 915–925.
13. Hosia, W., Johansson, J., and Griffiths, W. J. (2002) Hydrogen/deuterium exchange and aggregation of a polyvaline and a polyleucine  $\alpha$ -helix investigated by matrix-assisted laser desorption/ionization mass spectrometry, *Mol. Cell Proteomics* 1, 592–597.
14. Taddei, N., Capanni, C., Chiti, F., Stefani, M., Dobson, C. M., and Ramponi, G. (2001) Folding and aggregation are selectively influenced by the conformational preferences of the  $\alpha$ -helices of muscle acylphosphatase, *J. Biol. Chem.* 276, 37149–37154.
15. Tjernberg, L. O., Callaway, D. J., Tjernberg, A., Hahne, S., Lilliehook, C., Terenius, L., Thyberg, J., and Nordstedt, C. (1999) A molecular model of Alzheimer amyloid  $\beta$ -peptide fibril formation, *J. Biol. Chem.* 274, 12619–12625.
16. Azriel, R., and Gazit, E. (2001) Analysis of the minimal amyloid-forming fragment of the islet amyloid polypeptide. An experimental support for the key role of the phenylalanine residue in amyloid formation, *J. Biol. Chem.* 276, 34156–34161.
17. von Bergen, M., Barghorn, S., Li, L., Marx, A., Biernat, J., Mandelkow, E. M., and Mandelkow, E. (2001) Mutations of tau protein in frontotemporal dementia promote aggregation of paired helical filaments by enhancing local  $\beta$ -structure, *J. Biol. Chem.* 276, 48165–48174.
18. Richardson, J. S., and Richardson, D. C. (2002) Natural  $\beta$ -sheet proteins use negative design to avoid edge-to-edge aggregation, *Proc. Natl. Acad. Sci. U.S.A.* 99, 2754–2759.
19. Wang, W., and Hecht, M. H. (2002) Rationally designed mutations convert de novo amyloid-like fibrils into monomeric  $\beta$ -sheet proteins, *Proc. Natl. Acad. Sci. U.S.A.* 99, 2760–2765.
20. Tjernberg, L., Hosia, W., Bark, N., Thyberg, J., and Johansson, J. (2002) Charge attraction and  $\beta$  propensity are necessary for amyloid fibril formation from tetrapeptides, *J. Biol. Chem.* 277, 43243–43246.
21. Tjernberg, L. O., Tjernberg, A., Bark, N., Shi, Y., Ruzsicska, B. P., Bu, Z., Thyberg, J., and Callaway, D. J. (2002) Assembling amyloid fibrils from designed structures containing a significant amyloid  $\beta$ -peptide fragment, *Biochem. J.* 366, 343–351.
22. Hutchinson, E. G., and Thornton, J. M. (1994) A revised set of potentials for  $\beta$ -turn formation in proteins, *Protein Sci.* 3, 2207–2216.
23. Schuck, P. (2000) Size-distribution analysis of macromolecules by sedimentation velocity ultracentrifugation and lamm equation modeling, *Biophys. J.* 78, 1606–1619.
24. Totrov, M., and Abagyan, R. (1996) The contour-buildup algorithm to calculate the analytical molecular surface, *J. Struct. Biol.* 116, 138–143.
25. Bystrov, V. (1976) Spin–spin coupling and the conformational states of peptide systems, *Prog NMR Spectrosc.* 10, 41–81.
26. Wishart, D. S., Sykes, B. D., and Richards, F. M. (1991) Relationship between nuclear magnetic resonance chemical shift and protein secondary structure, *J. Mol. Biol.* 222, 311–333.
27. Watson, D. J., Selkoe, D. J., and Teplow, D. B. (1999) Effects of the amyloid precursor protein Glu693  $\rightarrow$  Gln Dutch mutation on the production and stability of amyloid  $\beta$ -protein, *Biochem. J.* 340, 703–709.
28. Rizzu, P., Joosse, M., Ravid, R., Hoogeveen, A., Kamphorst, W., van Swieten, J. C., Willemsen, R., and Heutink, P. (2000) Mutation-dependent aggregation of tau protein and its selective depletion from the soluble fraction in brain of P301L FTDP-17 patients, *Hum. Mol. Genet.* 9, 3075–3082.
29. Kraus, M., Janek, K., Bienert, M., and Krause, E. (2000) Characterization of intermolecular  $\beta$ -sheet peptides by mass spectrometry and hydrogen isotope exchange, *Rapid. Commun. Mass Spectrom.* 14, 1094–1104.

BI036248T